ARTICLE
Journal of Cellular Biochemistry 112:793–803 (2011)

Journal of Cellular Biochemistry

Bone Morphogenetic Protein 2 Signaling in Osteoclasts Is Negatively Regulated by the BMP Antagonist, Twisted Gastrulation

Lan Pham,[1] Kayla Beyer,[1] Eric D. Jensen,[1] Julio Sotillo Rodriguez,[1] Julia Davydova,[2] Masato Yamamoto,[3,4] Anna Petryk,[3,4] Rajaram Gopalakrishnan,[1*] and Kim C. Mansky[5**]

[1]*Department of Diagnostic and Biological Sciences, University of Minnesota School of Dentistry, Minneapolis, Minnesota 55455*

[2]*Department of Surgery, University of Minnesota Medical School, Minneapolis, Minnesota 55455*

[3]*Department of Genetics, Cell Biology and Development, University of Minnesota Medical School, 321 Church St. SE, Minneapolis, Minnesota 55455*

[4]*Department of Pediatrics, University of Minnesota Medical School, Minneapolis, Minnesota 55455*

[5]*Department of Developmental and Surgical Sciences, University of Minnesota School of Dentistry, Minneapolis, Minnesota 55455*

ABSTRACT

Bone morphogenetic proteins (BMPs) have been shown to regulate both osteoblasts and osteoclasts. We previously reported that BMP2 could directly enhance RANKL-mediated osteoclast differentiation by increasing the size and number of osteoclasts. Similarly, genetic deletion of the BMP antagonist Twisted gastrulation (TWSG1) in mice, resulted in an enhancement of osteoclast formation, activity and osteopenia. This was accompanied by increased levels of phosphorylated Smad (pSmad) 1/5/8 in *Twsg1*$^{-/-}$ osteoclasts in vitro. The purpose of this study was to develop an adenoviral vector overexpressing *Twsg1* as a means of inhibiting osteoclast activity. We demonstrate that overexpressing TWSG1 in primary osteoclasts decreased the size and number of multinuclear TRAP-positive osteoclasts, expression of osteoclast genes, and resorption ability. Overexpression of TWSG1 did not affect osteoclast proliferation or apoptosis. However, overexpression of TWSG1 decreased the levels of pSmad 1/5/8 in osteoclasts. Addition of exogenous BMP2 to osteoclasts overexpressing TWSG1 rescued the size and levels of pSmad 1/5/8 compared to cultures infected with a control virus. Finally, TWSG1 overexpression in osteoclasts isolated from the *Twsg1*$^{-/-}$ mice rescued size of the osteoclasts while further addition of exogenous BMP2 reversed the effect of TWSG1 overexpression and increased the size of the osteoclasts similar to control virus infected cells. Taken together, we demonstrate that overexpressing TWSG1 in osteoclasts via an adenoviral vector results in inhibition of osteoclastogenesis and may provide a potential therapy for inhibiting osteoclast activity in a localized manner. J. Cell. Biochem. 112: 793–803, 2011.

KEY WORDS: OSTEOCLAST; BONE MORPHOGENETIC PROTEIN 2; TWISTED GASTRULATION; BONE

Mammalian bone is under continuous remodeling in response to altered serum calcium levels, changes in mechanical loading, structural damage, and a wide range of paracrine and endocrine factors. Osteoclasts are derived from the monocyte/macrophage lineage and are formed by multiple cellular fusions from their mononuclear precursors [Vaananen and Laitala-Leinonen, 2008]. They initiate bone remodeling and resorb old bone. Altered osteoclast activity is an important component of various skeletal diseases. Thus, specific inhibition of osteoclast function has become a major strategy to treat osteolytic bone diseases such as osteoporosis, metastatic bone disease, arthritis, and other metabolic bone diseases [Rodan and Martin, 2000].

Bone morphogenetic proteins (BMPs) are multi-functional growth factors involved in numerous molecular cascades and signaling pathways. In addition to well-characterized actions on osteoblasts, BMPs are essential for osteoclast differentiation, but

Grant sponsor: National Institute of Dental and Craniofacial Research; Grant numbers: MinnCResT-T32, DE007288, R01 DE016601, R01CA094084, R03 DE020117, R01 AR056642.

*Correspondence to: Rajaram Gopalakrishnan, University of Minnesota School of Dentistry, 16-108A Moos Tower, 515 Delaware St SE, Minneapolis, MN 55455. E-mail: gopal007@umn.edu

**Correspondence to: Kim Mansky, University of Minnesota School of Dentistry, 6-320 Moos Tower, 515 Delaware Street SE, Minneapolis, Minnesota 55455. E-mail: kmansky@umn.edu

Received 30 July 2010; Accepted 8 November 2010 • DOI 10.1002/jcb.23003 • © 2010 Wiley-Liss, Inc.
Published online 14 December 2010 in Wiley Online Library (wileyonlinelibrary.com).

their role in the latter process remains incompletely characterized. Reports from our laboratory and others indicate that osteoclasts express BMP receptors and their ligands, BMP2 and BMP7 [Kanatani et al., 1995; Kaneko et al., 2000; Itoh et al., 2001; Jensen et al., 2010]. Treatment of osteoclasts with exogenous BMP2 directly enhances RANKL-stimulated differentiation of osteoclast precursors in vitro and stimulates survival and resorptive activity of mature osteoclasts [Kanatani et al., 1995; Kaneko et al., 2000; Itoh et al., 2001; Jensen et al., 2010]. Conversely, shRNA knockdown of BMPRII inhibits osteoclast formation [Jensen et al., 2010]. BMPs exert their biological activities by signaling through types I and II serine/threonine kinase transmembrane receptors [Itoh et al., 2001; Xiao et al., 2002; Nohe et al., 2004; Cao and Chen, 2005]. The signaling activity of BMPs is inhibited by secreted molecules such as Chordin (CHRD), Noggin, and Twisted gastrulation (TWSG1), which physically interact with BMPs and limit their ability to activate BMP receptors and downstream signaling pathways [Canalis et al., 2003].

Recently, we described a TWSG1-deficient (*Twsg1*$^{-/-}$) mouse which exhibited an osteopenic phenotype that was attributed to increased osteoclast formation and function [Rodriguez et al., 2009]. Osteoblast function was not affected in these mice, however, osteoclasts from *Twsg1*$^{-/-}$ mice were significantly larger and increased in number compared to osteoclasts from WT mice both in vitro and in vivo. Interestingly, the enhanced osteoclastogenesis phenotype seen in the *Twsg1*$^{-/-}$ mice could be recapitulated in osteoclasts from wild-type (WT) mice following treatment with exogenous recombinant BMP2 and suboptimal amounts of RANKL [Rodriguez et al., 2009]. Binding of BMPs to their receptor complex leads to phosphorylation of specific intracellular substrates such as receptor-regulated SMAD 1/5/8, whereas SMAD 2 and 3 mediate signaling for TGF-beta and the activins [Lieberman et al., 2002]. *Twsg1*$^{-/-}$ mice-derived osteoclasts had increased levels of phosphorylated SMAD (pSMAD) 1/5/8 consistent with increased BMP signaling due to loss of an antagonist [Rodriguez et al., 2009]. Collectively, these data suggest that TWSG1 attenuates BMP signaling in osteoclasts thereby functioning to limit osteoclast activity and bone remodeling.

The goal of the current study is to overexpress TWSG1 using an adenoviral vector to further characterize its role in osteoclastogenesis. We hypothesized that TWSG1 would inhibit osteoclastogenesis by inhibiting BMP signaling. Overexpressing TWSG1 in WT osteoclast precursors by adenovirus (Ad) transduction significantly reduced the size and activity of the differentiated osteoclasts. Addition of increasing amounts of exogenous BMP2 to TWSG1 overexpressing osteoclasts restored their size confirming the opposing activities of TWSG1 and BMP signaling in osteoclasts. Finally, we were able to rescue the increased size of *Twsg1*$^{-/-}$ osteoclasts by infecting them with the TWSG1 expressing Ad.

MATERIALS AND METHODS

MICE

Generation and genotyping of *Twsg1*$^{-/-}$ mice were previously described [Petryk et al., 2004]. The use and care of the mice in this study was approved by the University of Minnesota Institutional Animal Care and Use Committee.

PRIMARY OSTEOCLAST CULTURES

Femoral and tibial bone marrow cells were collected from 4-week-old WT or *Twsg1*$^{-/-}$ mice in the 129Sv/Ev background. The tibiae and femora were removed and dissected free of adhering tissues. The bone ends were removed and the marrow cavities flushed by slowly injecting media through one end using a 25-gauge needle. The flushed bone marrow cells were cultured for 3 days on non-tissue culture coated dishes in phenol red-free α-MEM supplemented with 5% heat-inactivated fetal bovine serum, 25 U/ml penicillin, 400 mM L-glutamine, and 10 ng/ml M-CSF (R&D Systems). The adherent cell population, containing the committed osteoclast precursors, was re-plated at 2×10^4 cells/cm^2 in osteoclast media further supplemented with 60 ng/ml RANKL (R&D Systems) and/or BMP2 (R&D Systems) as indicated. Osteoclast resorption assay was performed on dentine discs (Immunodiagnostic Systems) in triplicate. Dentine discs were stained with toluidine blue to visualize resorption pits. Resorption area was observed with light microscopy, photographed, and measured using NIH Image J.

CONSTRUCTION OF ADENOVIRUS EXPRESSING TWSG1

The adenovirus type 5 (Ad5) vector expressing full-length *Twsg1* cDNA (Ad-T or Ad-Twsg1) contains the CMV promoter-driven *Twsg1* transgene cassette inserted in place of the deleted E1 region of a common Ad5 vector. The full-length *Twsg1* cDNA expressed in pCMV-Tag 4A vector (*Not*I and *Bam*HI sites) was cloned into pShuttleCMV plasmid [Davydova et al., 2004] using the *Not*I and *Bgl*II sites. The resultant plasmid, pShuttleCMV-*Twsg1*, was linearized with *Pme*I digestion and subsequently co-transformed into *E. coli* BJ5183 with the RGD fiber-modified Ad backbone plasmid (RGDAdEasy). After selection of recombinants, the recombinant DNA was linearized with *Pac*I digestion and transfected into 911 cells to generate Ad-T. The virus was propagated in 293T cells, dialyzed in phosphate-buffered saline (PBS) with 10% glycerol, and stored at −80°C. Titering was performed with a plaque-forming assay using 911 cells (pfu/ml) and optical density-based measurement (Vp/ml). An identical replication-incompetent CMV promoter-driven luciferase expression vector (Ad-C) was used as a control vector. Detailed information about procedures taken to construct the RGD fiber-modified Ad5 backbone plasmid (RGDAdEasy) and Ad-C control vector is available upon request.

ADENOVIRUS INFECTION OF OSTEOCLASTS

Primary bone marrow cells treated with M-CSF for 3 days on non-tissue culture coated plates were plated in 12-well plate (2.5×10^5 cells/well). Twenty-four hours after plating the osteoclasts, the cells were incubated with 10 multiplicity of infection (MOI) of either Ad-T or Ad-C for 3 h at 37°C in the presence of M-CSF and RANKL. After 3 h, the Ad vector was removed from the osteoclasts and the cells were treated with M-CSF, RANKL, and where indicated in the figure legends BMP2 was added to the osteoclast differentiation media. MOI was calculated using the pfu/

ml measurement. On day 3 post-infection, total mRNA was extracted for gene expression by real-time RT-PCR or protein was extracted for Western blots. Luciferase activity was determined with the Luciferase Assay System (Promega) 48 h post-infection. Experiments were performed in triplicate and normalized to protein concentration (BioRad).

TRAP STAINING

Seven days post-infection primary osteoclasts were fixed in 4% paraformaldehyde (PFA). Fixed cells were washed by PBS and stained with acid phosphoric reagents with tartrate [5 mg Napthol AS-MX phosphate, 0.5 ml *N*,*N*-dimethyl formamide, 50 ml acetic acid buffer (1 ml acetic acid, 6.8 g sodium acetate trihydrate, 11.5 g sodium tartarate in 1 L water), and 25 mg Fast Violet LB salt]. Triplicate samples were used.

HISTOMORPHOMETRIC ANALYSIS OF OSTEOCLASTS

Osteoclasts that had been stained with TRAP were photographed at 10× magnification. After cells were TRAP stained and photographed, cells were stained with DAPI (Molecular Probes) for 5 min at room temperature. Cells were photographed again at 10× magnification. Images were overlaid in Adobe Photoshop and all the TRAP-positive cells containing three or more nuclei were counted and measured using NIH Image J. Experiments were done in triplicate by counting all the positive cells in three wells.

REAL-TIME RT-PCR

Total RNA was isolated from cells using TRIzol reagent (Invitrogen) and quantitated by UV spectroscopy. cDNA was synthesized using 2 μg of RNA and the iScript cDNA Synthesis kit (Bio-Rad). PCR reactions, data quantification, and analysis were performed using MyiQ Single-Color real-time PCR Detection System (Bio-Rad). Values were normalized to *L4* mRNA. Primer sequences used were NFATc1 (Forward) 5′-TCA TCC TGT CCA ACA CCA AA; (Reverse) 5′-TCA CCC TGG TGT TCT TCC TC; Cathepsin K (Forward) 5′-AGG GAA GCA AGC ACT GGA TA; (Reverse) 5′-GCT GGC TGG AAT CAC ATC TT; DC-STAMP (Forward) 5′-GGG CAC CAG TAT TTT CCT GA; (Reverse) 5′-TGG CAG GAT CCA GTA AAA GG; Twsg1 (Forward) 5′-ATG AAG TCA CAC TAT ATT; (Reverse) 5′-CTG AAT GAG GCA TTT GCT CA. All measurements were performed in triplicate and analyzed using the $2^{-\triangle\triangle Ct}$ method.

IMMUNOFLUORESCENCE

To visualize expression of TWSG1 in osteoclasts, cells were grown on glass cover slips and fixed in 4% PFA for 20 min. The cells were then permeabilized in PBS/0.3% Triton X-100 for 5 min, blocked in immunofluorescence buffer (3% BSA, 20 mM $MgCl_2$, 0.3% Tween-20 in PBS) for 20 min, and incubated with primary antibodies for 90 min in immunofluorescence buffer. Anti-mouse TSG antibody (R&D Systems) was used at 1:200. Cells were washed three times in PBS/0.1% Triton X-100, and then incubated for 30 min with Alexa-conjugated secondary antibodies at 1:800 (Invitrogen). After three washes, cells were stained with DAPI, washed, and mounted in 90% glycerol/0.4% *N*-propyl-gallate. Images were obtained using an Olympus Fluoview 500 confocal microscope.

IMMUNOBLOTTING

Cell protein lysates were prepared in modified RIPA lysate supplemented with protease inhibitor (Roche) and phosphatase inhibitor cocktails (Sigma–Aldrich). Crude lysates were sonicated and cleared by centrifugation at 12,000 rpm at 4°C. Proteins were resolved by SDS–PAGE, transferred to PDVF membrane (Millipore) and incubated overnight at 4°C with primary antibodies against pSMAD 1/5/8 (Cell Signaling), total SMAD 1/5/8 (Santa Cruz), Caspase-3 (Cell Signaling), α-tubulin (Cell Signaling), and appropriate horseradish peroxidase-conjugated secondary antibodies (Santa Cruz). Polyclonal antibody to mouse TWSG1 was generated by Thermo Fisher Scientific Open Biosystems (Huntsville, AL). Immunoreactive bands were visualized using ECL Plus substrate (GE Health Systems).

PROLIFERATION ASSAY

Primary osteoclast cells were plated at 3×10^4 cells/well in 48-well plate and cultured in α-MEM containing 10% FBS and 50 ng/ml M-CSF (R&D Systems). Cells were stimulated with 60 ng/ml RANKL (R&D Systems) and infected with either Ad-C or Ad-T. Each condition was performed in triplicate. Each day osteoclast proliferation was assessed by CellTiter 96 Aqueous One Solution Cell Proliferation kit (Promega) according to the manufacturer's instructions. Absorbance was recorded at 490 nm.

STATISTICAL ANALYSIS

All experiments were run in triplicates and results are expressed as mean ± SD. One-way ANOVA with a Tukey post hoc test was used to compare data; $P < 0.05$ indicates significance.

RESULTS

EXPRESSION OF TWSG1 IN OSTEOCLASTS

We previously showed that *Twsg1* is expressed in differentiated osteoclasts [Rodriguez et al., 2009]. To further define *Twsg1* expression throughout osteoclast differentiation, we performed real-time RT-PCR to measure *Twsg1* mRNA expression in osteoclast precursors undergoing RANKL-stimulated differentiation. *Twsg1* mRNA was present in osteoclasts at day 0 and increased as they matured (Fig. 1A). Immunofluorescence against TWSG1 confirmed the presence of TWSG1 protein located throughout the cytoplasm during all stages of osteoclast differentiation (Fig. 1B). Other cells in our bone marrow cultures could also be expressing TWSG1 namely osteoblasts and/or stromal cells [Petryk et al., 2005]; however, it is evident from our immunofluorscence data that by day 5 multinuclear osteoclasts are expressing TWSG1.

CONSTRUCTION OF ADENOVIRUS EXPRESSING FULL-LENGTH TWSG1

We previously showed that osteoclasts from mice deficient for TWSG1 were larger in size than osteoclasts from WT mice [Rodriguez et al., 2009]. To determine the phenotype of osteoclasts when TWSG1 is overexpressed, we generated an Ad that expresses full-length *Twsg1* (Ad-TWSG1 or Ad-T).

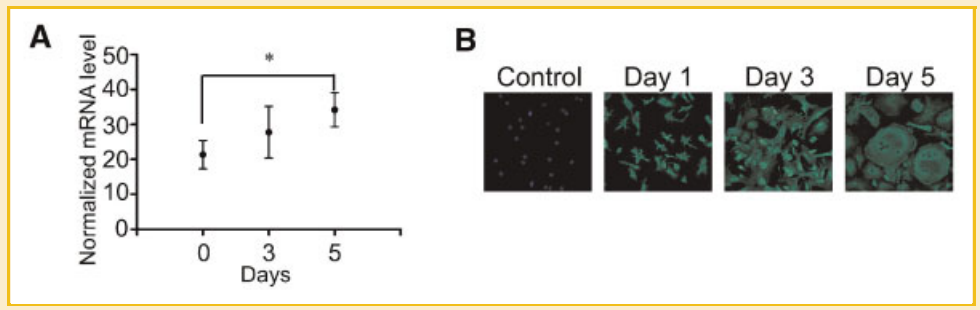

Fig. 1. Expression of Twsg1 during osteoclast differentiation. A: Expression profile of *Twsg1* mRNA from M-CSF (day 0) and M-CSF + RANKL-treated osteoclast cultures (days 3 and 5). $^{*}P \leq 0.01$ day 0 compared to day 5. B: TWSG1 immunofluorscence staining (green) of 1, 3, and 5 days osteoclast cultures. Cells were co-stained with DAPI (dark blue) to show cell nuclei. Parallel slides from each day were stained without TWSG antibody as a negative control (control).

The efficiency of Ad-mediated gene transfer largely depends on the biology of the virus-cell interaction: the initial high-affinity binding of Ad to the primary Coxsackie-adenovirus receptor (CAR) and the interaction between Arg-Gly-Asp (RGD) motifs in the Ad penton base protein and the integrin molecules on the cell surface. To obtain the most effective transduction in osteoclasts, we sought to determine whether adenoviral vectors equipped with different genetically modified fibers would overcome low-transduction efficiency of CAR-deficient cells [Davydova et al., 2004]. We infected bone marrow cultures with either 100 or 1,000 Vp/cell of

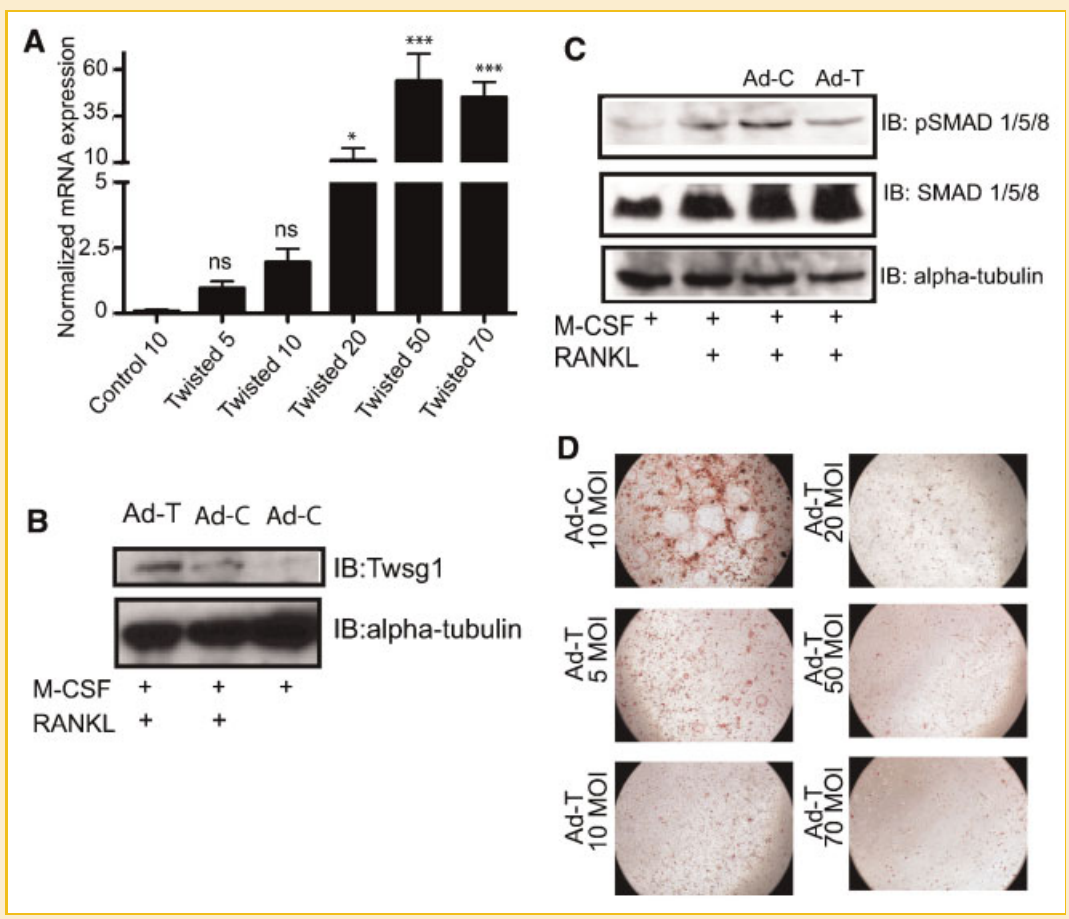

Fig. 2. Characterization of TWSG1 expressing adenovirus. A: Real-time RT-PCR analysis of *Twsg1* expression from osteoclasts infected with Ad-TWSG1 at increasing MOIs. Osteoclasts were harvested after incubation with RANKL for 3 days. $^{*}P \leq 0.01$ control compared to Twisted 20, $^{***}P \leq 0.0001$ control compared to TWSG1 50 and 70, ns = not significant. B: Immunoblot analysis of osteoclast precursors infected with Ad-TWSG1 at an MOI of 10. C: Immunoblot analysis of osteoclast precursors showing levels of phosphorylated SMAD 1/5/8 and total SMAD 1/5/8 and alpha-tubulin as a loading controls in Ad-C- or Ad-TWSG1-infected osteoclasts. Osteoclasts were harvested after 4 days in the presence of RANKL. D: TRAP staining of 7-day osteoclast cultures infected with the indicated MOI of Ad-TWSG1.

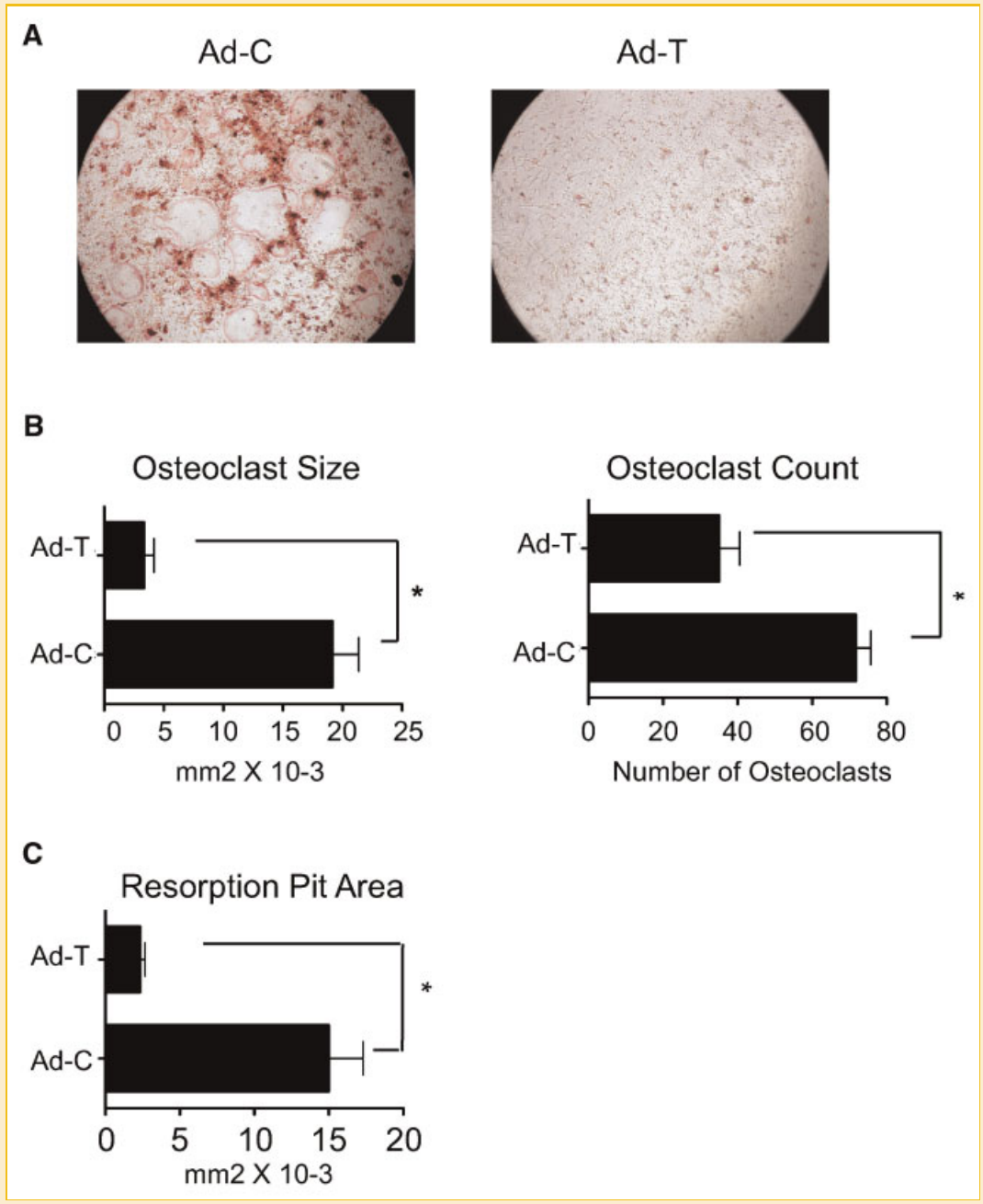

Fig. 3. TWSG1 overexpression inhibits osteoclastogenesis. A: TRAP staining of 7-day osteoclast cultures infected with Ad-C or Ad-TWSG1 (Ad-T) at 10 MOI. Note that these are larger images of the cells shown in Figure 2D. B: Histomorphometric analysis of TRAP-stained osteoclasts. $^{*}P < 0.05$ compared to Ad-C. TRAP-positive osteoclasts containing three or more nuclei were counted. C: Quantification of resorption pit area of toluidine blue stained dentine disks. Osteoclasts were incubated in the presence of RANKL for 10 days. $^{*}P < 0.05$ compared to Ad-C.

fiber-unmodified Ad (Unmod Ad), RGD Ad which has a RGD-4C peptide inserted in the H1 loop of the Ad5 fiber knob, CpK Ad which has a polylysine motif inserted in the Ad5 fiber gene, or 5/3 Ad which expresses a chimeric fiber composed of the Ad5 shaft and the Ad type 3 knob. All of these Ads express luciferase reporter gene and are identical except for their genetically modified fibers [Davydova et al., 2004]. We found that bone marrow cultures infected with the RGD or the CpK modified Ad at 100 Vp/cell expressed greater luciferase activity compared to either unmodified or the 5/3 Ad construct. It has been reported that RGD modification allows the Ad to use the cellular integrins, thus remarkably increasing the viral infectivity in many cells [Davydova et al., 2004]. Based on this report and our observation, we further constructed the TWSG1 expressing Ad5 armed with RGD-modified fiber and applied them to bone marrow cultures.

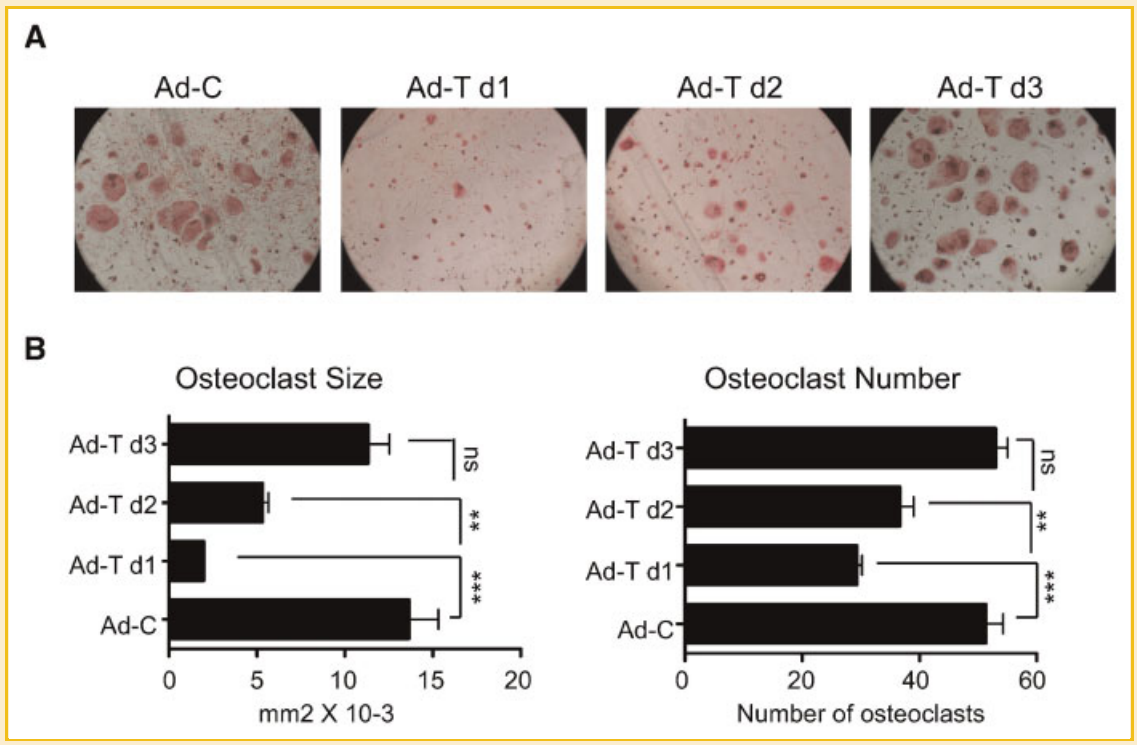

Fig. 4. TWSG1 inhibits osteoclastogenesis on days 1–2 after RANKL addition. A: TRAP staining of 7-day osteoclast cultures infected with either Ad-C or Ad-TWSG1 at 1 day (d1), 2 days (d2), or 3 days (d3) after the addition of RANKL to the cultures. B: Histomorphometric analysis of TRAP-stained osteoclasts. TRAP stained osteoclasts with three or more nuclei were counted. $^{**}P \leq 0.01$ Ad-C compared to Ad-Td2 and $^{***}P \leq 0.0001$ Ad-C compared to Ad-d1, ns = not significant.

CHARACTERIZATION OF TWSG1 EXPRESSING AD

We confirmed that *Twsg1* mRNA expression increased in osteoclasts proportionally to increasing MOI (Fig. 2A). Furthermore, we demonstrated by Western blot that osteoclast-like cells infected with an MOI of 10 of Ad-*Twsg1* express more TWSG1 than control infected cells treated with M-CSF alone or M-CSF + RANKL (Fig. 2B). Because TWSG1 has been previously shown to function as a BMP antagonist in vertebrate systems [Ross et al., 2001; Nosaka et al., 2003; MacKenzie et al., 2009], we determined whether BMP signaling was reduced by overexpression of TWSG1 in osteoclasts. We found reduced levels of pSMAD 1/5/8 in TWSG1 overexpressing osteoclasts compared to Ad-C infected osteoclasts (compare lanes Ad-C to Ad-T, Fig. 2C). These observations indicated that infection of osteoclasts with Ad-T results in increased TWSG1 expression and decreased BMP signaling as expected.

TWSG1 INHIBITS OSTEOCLASTOGENESIS

We began our characterization of the effect of TWSG1 overexpression on osteoclastogenesis by infecting osteoclast precursors with increasing amounts of the adenoviral vectors, stimulating differentiation by treatment with M-CSF and RANKL, and assessing the resulting multinucleated osteoclasts by TRAP staining. Osteoclasts infected with Ad-T at an MOI of 5 were notably smaller than Ad-C infected cells at the same MOI. Increasing the MOI of Ad-T to 10 gave a strong decrease in OCL size that was not further reduced at higher levels of infection (Fig. 2D). Because an MOI of 10 was the lowest level to give the maximal effect, this level of infection was used in all subsequent experiments.

Quantitative analysis indicated that an MOI of 10, TWSG1 overexpressing osteoclast cultures (Fig. 3A) displayed a significant reduction in the number of TRAP-positive multinucleated cells (Fig. 3B). Further these cells had an average size of approximately 0.003 mm^2 while Ad-C infected cells were significantly larger, averaging 0.015 mm^2 (Fig. 3B). For determination of osteoclast size and number only TRAP-positive osteoclasts containing three or more nuclei were measured. Ad-T-infected osteoclasts also exhibited significantly less resorptive ability when plated on dentine substrates (Fig. 3C). These observations demonstrate that TWSG1 overexpression inhibits osteoclast formation and function.

TWSG1 INHIBITS OSTEOCLAST FORMATION ON DAYS 1 AND 2

We have previously shown that addition of exogenous BMP2 to osteoclast cultures on the 3rd day after the addition of RANKL enhances formation of TRAP-positive cells [Jensen et al., 2010]. To determine the effects of overexpressing *Twsg1* in osteoclasts at different times after addition of RANKL, infections were performed on osteoclasts at different days of differentiation and then the cultures were TRAP stained. TRAP analysis shows that there was a significant difference in size and number of osteoclasts when virus was added on day 1 or 2 after the addition of RANKL compared to cells infected with either the control virus or when virus was added on day 3 after the addition of RANKL (Fig. 4). However, there was no

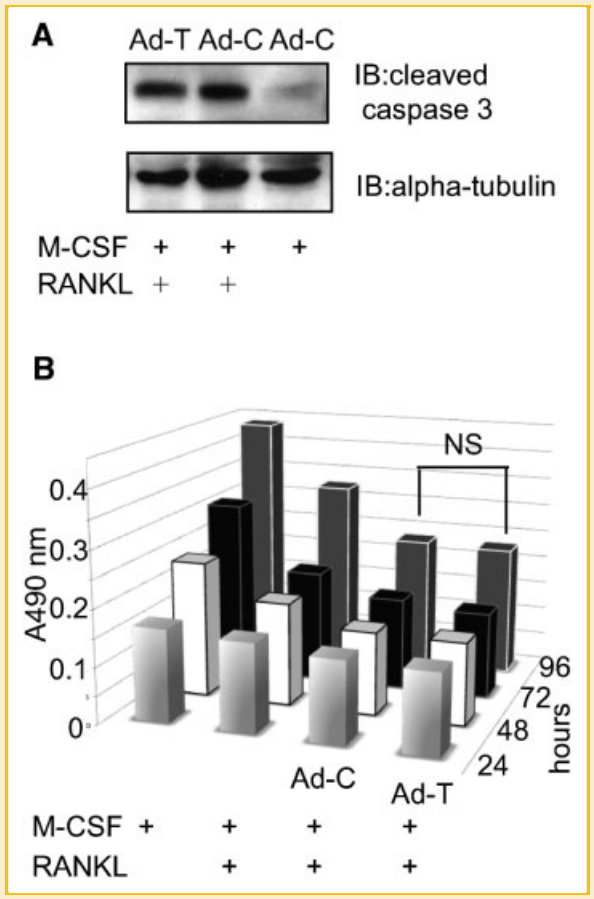

Fig. 5. Overexpressing TWSG1 does not affect osteoclast apoptosis or proliferation. A: Immunoblot analysis of cleaved caspase-3 levels and α-tubulin as a loading control from Ad-C- or Ad-TWSG1-infected osteoclast cultures. Osteoclast cultures were incubated in the presence of RANKL for 3 days. B: Bone marrow cultures were infected with Ad-C or Ad-TWSG1 adenovirus and treated as indicated. Cell number was determined on each day from triplicate samples using the Cell Titer 96 Aqueous One Solution Assay. ns = not significant.

significant change in the number or size of TRAP-positive osteoclasts compared to the osteoclasts infected with the control virus when virus was added 3 days after the addition of RANKL (Fig. 4B, compare Ad-C and Ad-T d3).

TWSG1 DOES NOT ALTER APOPTOSIS OR PROLIFERATION OF OSTEOCLASTS

One possible explanation for the impaired osteoclast formation in TWSG1 overexpressing cultures is that TWSG1 either induced cell death or interfered with cell proliferation. Cleavage of caspase-3 is a crucial step of programmed cell death [Porter and Janicke, 1999]. We observed an increase of cleaved caspase-3 in cells treated with RANKL (Fig. 5A), which is consistent with earlier work demonstrating that RANKL can induce apoptosis [Bharti et al., 2004]. Importantly, no difference was observed in the amount of cleaved caspase-3 between osteoclasts infected with Ad-C or Ad-T (Fig. 5A, compare Ad-C + RANKL and Ad-T + RANKL). This suggests that Ad-T does not induce more apoptosis than that observed in cells infected with the Ad-C and the decrease in formation of TRAP-positive multinuclear cells seen in Figure 3 is most likely not due to the osteoclasts undergoing apoptosis.

We next tested whether the effects of TWSG1 overexpression could result from decreased proliferation of osteoclast precursors. Osteoclast cultures were treated with M-CSF alone, M-CSF + RANKL, M-CSF + RANKL + Ad-C, or M-CSF + RANKL + Ad-T. Cell number was determined using an MTS-based assay after 24, 48, 72, and 98 h. We observed a slight decrease in proliferation when RANKL was added to the cells (Fig. 5B), which is consistent with work done by others demonstrating that RANKL can suppress cell propagation [Bharti et al., 2004]. Interestingly, infecting osteoclasts with Ad-T does not interfere with osteoclast proliferation when compared to Ad-C (Fig. 5B). These results suggest that TWSG1 overexpression does not inhibit osteoclast formation by affecting proliferation.

TWSG1 REDUCES OSTEOCLAST GENE EXPRESSION

Real-time RT-PCR validated the enhanced expression of *Twsg1* (approximately fivefold increase compared to Ad-C + RANKL) in infected cultures but also revealed a marked reduction in osteoclast markers (Fig. 6, compare Ad-C + RANKL and Ad-T + RANKL): *Nfatc1* (twofold decrease compared to Ad-C + RANKL, $P < 0.05$), *Cathepsin K* (*Ctsk*, twofold decrease compared to Ad-C + RANKL, $P < 0.05$), and *DC-STAMP* (2.5-fold decrease compared to Ad-C + RANKL, $P < 0.05$). These data suggest that TWSG1 is affecting osteoclast differentiation by changing gene expression.

BMP2 RESCUES TWSG1 OVEREXPRESSING OSTEOCLASTS

If TWSG1 inhibits osteoclast formation by inhibiting BMP signaling, we predicted that addition of BMP2 should rescue the osteoclast phenotype of TWSG1 overexpression. Osteoclast cultures were infected with Ad-C or Ad-T, followed by treatment with RANKL and either 20 ng/ml (low dose) or 80 ng/ml (high dose) of BMP2. As was previously described, TWSG1 overexpression reduced pSMAD 1/5/8 levels. However, addition of increasing amounts of BMP2 increased pSMAD 1/5/8 levels (Fig. 7A, compare Ad-T, Ad-T + 20, or Ad-T + 80 ng/ml BMP2). When cells were treated in this manner and stimulated to undergo differentiation with RANKL, BMP2 restored both the number and size of multinucleated TRAP-positive osteoclasts (Fig. 7B). However, while BMP2 treatment increased the expression of osteoclast markers, *Nfatc1*, *Ctsk*, and *DC-STAMP* in a dose-dependent manner, the change was not statistically significant compared to Ad-*Twsg1* (Ad-T) infected cells (Fig. 7E compare 3 with 4–5). The addition of BMP2 had no effect on *Twsg1* expression (Fig. 7C,D).

TWSG1 OVEREXPRESSION RESCUES THE IN VITRO OSTEOCLAST PHENOTYPE FROM TWSG1 NULL MICE

At the same time as osteoclasts from WT mice were being infected with the Ad-T (Fig. 7), we also infected littermates who were deficient in TWSG1 to determine if TWSG1 overexpression could rescue the enhanced osteoclastogenesis in *Twsg1*$^{-/-}$ primary osteoclasts. TWSG1 overexpression rescued the *Twsg1*-knockout phenotype by restoring the infected osteoclasts to both size and

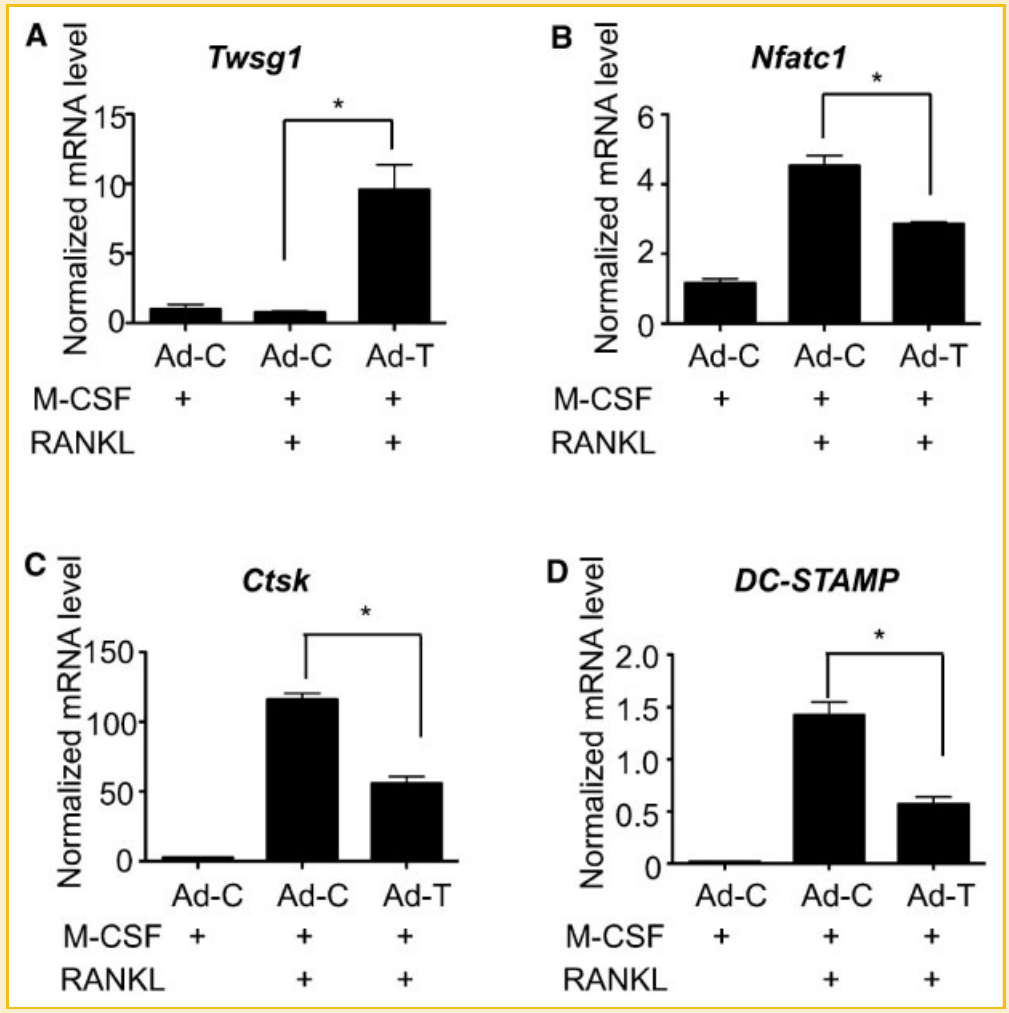

Fig. 6. Regulation of osteoclast gene expression and activity by TWSG1. Expression profile of (A) *Twsg1*, (B) *Nfat-c1*, (C) *Ctsk*, and (D) *DC-STAMP* mRNA from osteoclast cultures infected with Ad-C or Ad-T. Osteoclast cultures were incubated in the presence of RANKL for 3 days. $^{*}P \leq 0.05$ compared to Ad-C.

number similar to that of WT cells (Fig. 8, compare lane Ad-C to Ad-T). Further, the rescue of *Twsg1*$^{-/-}$ osteoclasts by TWSG1 overexpression was reversed by addition of increasing amounts of BMP2, which progressively increased both osteoclast size and number; however, the increases seen with the addition of exogenous BMP2 were not statistically significant when compared to cells infected with the TWSG1 overexpressing Ad (Fig. 8, compare Ad-T with Ad-T + B20 and Ad-T + B80). These results confirm that the phenotype of *Twsg1*$^{-/-}$ osteoclasts arises due to up-regulated BMP signaling, loss of TWSG1 expression and indicate that the balance between pro- and anti-BMP activities regulates osteoclast size.

DISCUSSION

We previously showed that osteoclasts from mice deficient for TWSG1 were more numerous and larger than osteoclasts from their WT littermates [Rodriguez et al., 2009]. In the current report, we present experiments that confirm the inhibitory role of TWSG1 in osteoclast differentiation. We show that *Twsg1* is expressed in osteoclasts at all stages during differentiation both by real-time PCR and immunofluorescence. Overexpression of TWSG1 significantly decreased both the size and number of multinuclear TRAP-positive cells and inhibited pSMAD 1/5/8 signaling. Conversely, addition of exogenous BMP2 rescued the diminished osteoclast phenotype following TWSG1 overexpression. These results are consistent with our previous data in which treatment of osteoclasts with Noggin inhibited their differentiation [Rodriguez et al., 2009; Jensen et al., 2010]. Thus, experiments using either Noggin or TWSG1 indicate that decreased BMP signaling impairs osteoclast fusion. The hypothesis that expression of TWSG1 impairs osteoclast fusion was supported by data showing that proliferation and apoptosis were not different in osteoclasts infected with Ad-T compared to Ad-C (Fig. 5). The proliferation and apoptosis data indicate that the number of osteoclast precursors was not increased or decreased but that the reduced multinuclear TRAP-positive osteoclasts was due to less fusion of the precursors. Taken together our data further supports the hypothesis that TWSG1 negatively regulates osteoclastogenesis by disrupting pro-osteoclastic BMP signaling.

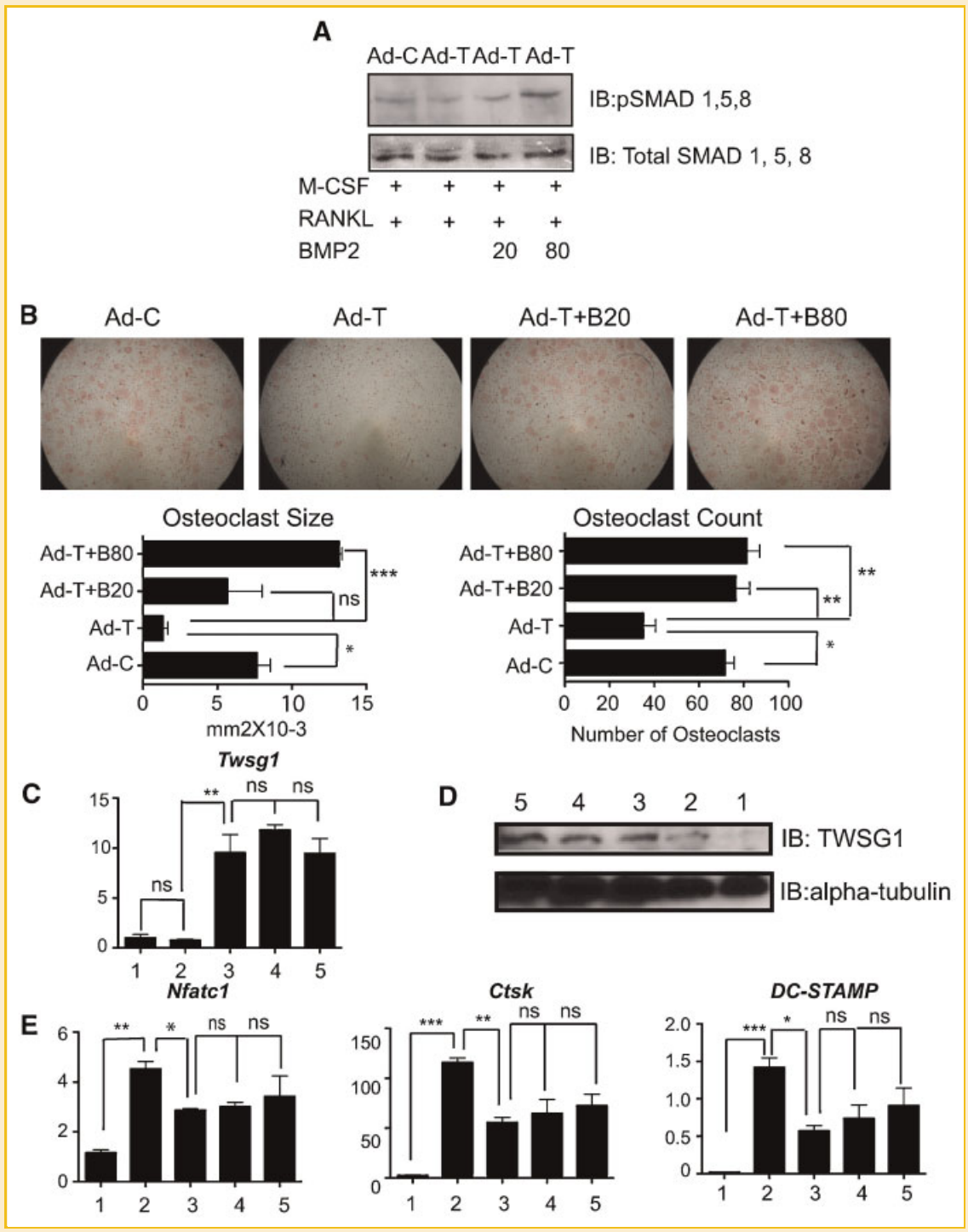

Fig. 7. BMP2 reverses the effects of TWSG1 overexpression. A: Immunoblot analysis of osteoclast precursors showing protein expression of levels of pSMAD 1/5/8 in Ad-C or Ad-TWSG1 osteoclasts and treated with BMP2 where indicated. Osteoclasts were incubated in the presence of RANKL and BMP2 for 3 days. B: TRAP staining and histomorphometry of 7-day osteoclast cultures infected with Ad-C or Ad-TWSG1. Where indicated in the figure osteoclasts were also treated with either 20 or 80 ng/ml of recombinant BMP2. TRAP-positive osteoclasts with three or more nuclei were counted. $^{*}P < 0.05$ compared to Ad-C, $^{**}P < 0.001$, and $^{***}P < 0.0001$ compared to Ad-T, ns = not significant (C) and (D) Expression profile of *Twsg1* mRNA and protein from osteoclast cultures infected with Ad-C (1), Ad-C + RANKL (2), Ad-T + RANKL (3), Ad-T + RANKL + BMP2 (20 ng/ml) (4), or Ad-T + RANKL + BMP2 (80 ng/ml) (5). Osteoclasts were incubated in the presence of RANKL and BMP2 for 3 days. $^{**}P < 0.001$ comparing Ad-T + RANKL (bar 3) to Ad-C + RANKL (bar 2). ns = Not significant when comparing Ad-C + RANKL (bar 2) and Ad-C + M-CSF (bar 1) and Ad-T + B20 (bar 4) or Ad-T + B80 (bar 5) to Ad-T (bar 3). E: Expression profile *Nfat-c1*, *Ctsk*, and *DC-STAMP* mRNA from osteoclast cultures infected with Ad-C (1), Ad-C + RANKL (2), Ad-T + RANKL (3), Ad-T + RANKL + BMP2 (20 ng/ml) (4), or Ad-T + RANKL + BMP2 (80 ng/ml) (5). Osteoclasts were incubated in the presence of RANKL and BMP2 for 3 days. $^{*}P < 0.05$, $^{**}P < 0.001$, and $^{***}P < 0.0001$ compare lane 1 to lane 2 or lane 2 to lane 3, ns = not significant.

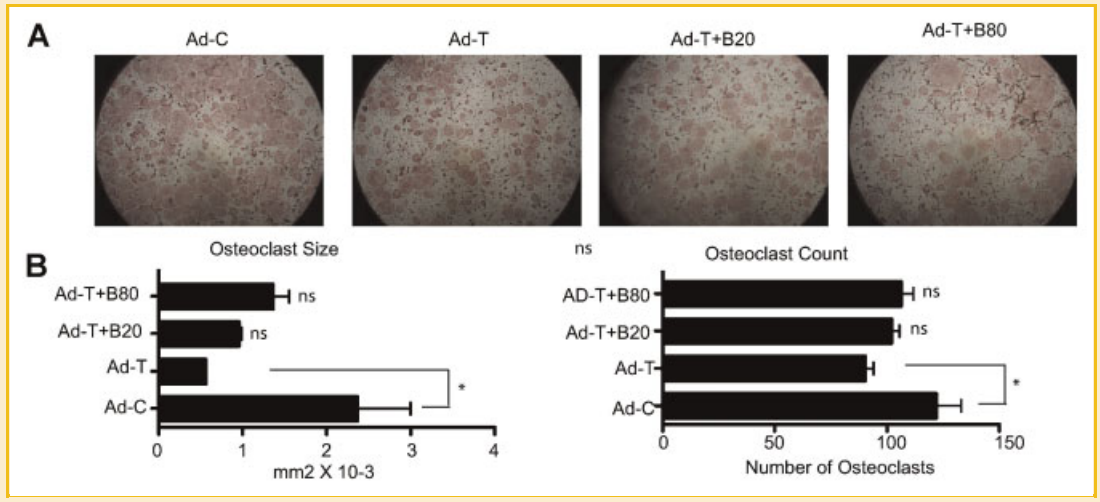

Fig. 8. Antagonistic activity of TWSG1 overexpression and BMP2 on *Twsg1*$^{-/-}$ osteoclasts. TRAP staining and histomorphometry of 7-day osteoclast cultures from *Twsg1*$^{-/-}$ mice infected with Ad-C or Ad-TWSG1. Where indicated in the figure osteoclasts were also treated with either 20 or 80 ng/ml of recombinant BMP2. TRAP-positive osteoclasts with three or more nuclei were counted. $^{*}P < 0.05$ compared to Ad-C, ns = not significant.

The balance between bone formation and resorption at sites of bone remodeling is regulated by autocrine and paracrine factors such as BMPs. While it is well established that BMPs enhance bone formation through multiple mechanisms, the significance of BMP signaling on osteoclasts is not as clear. However, a growing body of studies including our own demonstrate that BMPs directly influence the differentiation and the activity of osteoclasts [Kanatani et al., 1995; Kaneko et al., 2000; Itoh et al., 2001; Okamoto et al., 2006; Giannoudis et al., 2007; Jensen et al., 2010]. In addition to multiple important physiological roles in regulating bone formation, BMPs are used clinically to promote localized bone growth and healing in a number of orthopedic and maxillofacial applications [Kirker-Head et al., 2007]. In vivo application of BMPs during orthopedic procedures has been found to promote a transient increase in osteoclast numbers and osteoclastic bone resorption in some instances [Toth et al., 2009]. Our data provide a mechanistic explanation for this clinical observation and suggest rational strategies to minimize inappropriate activation of osteoclasts in this context and in other pathological skeletal conditions.

In our present study, we show that TWSG1 overexpression inhibits RANKL-induced osteoclast differentiation. Consistent with this, we previously showed that BMP2 treatment of osteoclasts enhanced RANKL-stimulated osteoclast differentiation, although BMP2 did not support differentiation in the absence of RANKL [Rodriguez et al., 2009; Jensen et al., 2010]. The precise mechanism by which BMP signaling regulates osteoclasts remains unknown; from our data we speculate that BMP signals may influence responses to RANKL signaling.

TWSG1 has been previously shown to act as a BMP antagonist in vertebrates, although there is some evidence for an agonist function as well [Larrain et al., 2001; Ross et al., 2001; Nosaka et al., 2003; Oelgeschlager et al., 2003; MacKenzie et al., 2009]. After 3 days in the presence of RANKL, osteoclasts infected with Ad-T were still able to differentiate. We hypothesize that BMP signaling is critical during an early stage of osteoclast differentiation. We were able to rescue the osteoclast phenotype following overexpression of TWSG1 by adding increasing amounts of BMP2. We also report that overexpression of TWSG1, rescues the in vitro osteoclast phenotype in *Twsg1*$^{-/-}$ mice. As further confirmation of TWSG1's role in regulating BMP signaling, we were again able to reverse the reduction in size seen with TWSG1 infection. These results suggest that BMP-signaling directly promotes the differentiation of mature osteoclasts and further clarifies a novel anti-resorptive function for TWSG1 by modulating BMP-signaling.

TWSG1 has been shown in other invertebrate and vertebrate systems to act as a BMP antagonist by forming a ternary complex with CHRD, a cysteine-rich (CR) protein, and BMPs, Other CR proteins have been shown to modulate TGF-β/BMP signaling and these CR proteins may also modulate TWSG1's interaction with BMPs [Larrain et al., 2001; Ross et al., 2001; Oelgeschlager et al., 2003]. It is not known if the mechanism by which TWSG1 inhibits BMP signaling during osteoclast differentiation is through its interaction with CHRD or other CR proteins.

Due to their ability to inhibit bone resorption, bisphosphonates are widely used effectively to treat widespread osteolytic bone diseases such as osteoporosis and metastatic bone disease. However, bisphosphonates are less desirable for treatment of localized osteolytic diseases such as periodontitis. Therefore, local delivery of genes that can inhibit osteoclast function may provide an effective alternate. Gene therapies rely on the delivery of foreign DNA into cells. This has led to the engineering of efficient delivery systems, such as Ad, retroviruses, or lentiviruses into cells. Traditional viral systems, including retrovirus and lentivirus systems, have limited therapeutic use as their DNA integrates into the host genome, which may cause unwanted side effects. Using a robust adenoviral delivery systems to administer TWSG1 transiently, locally, and non-evasively to the cells or tissues may prove to be an efficient and clinically relevant anti-resorptive tool to combat local aberrant bone loss. Specifically, the use of an RGD-modified Ad system, like the one used in this report, could have the additional

advantages that it allows for lower vector dose to achieve similar therapeutic effects while preventing inflammatory responses to the vector. Here, we demonstrate that overexpressing TWSG1 to osteoclasts in vitro via an RGD adenoviral construct results in an inhibition of osteoclast formation.

ACKNOWLEDGMENTS

This project was supported in part by R01 DE016601 to A.P., R01 CA094084 to M.Y., and R01 AR056642 to R.G., R03 DE020117 to E.J., MinnCResT-T32 DE007288 to L.P. and J.S.R. from the National Institute of Dental and Craniofacial Research.

REFERENCES

Bharti AC, Takada Y, Shishodia S, Aggarwal BB. 2004. Evidence that receptor activator of nuclear factor (NF)-kappaB ligand can suppress cell proliferation and induce apoptosis through activation of a NF-kappaB-independent and TRAF6-dependent mechanism. J Biol Chem 279:6065–6076.

Canalis E, Economides AN, Gazzerro E. 2003. Bone morphogenetic proteins, their antagonists, and the skeleton. Endocr Rev 24:218–235.

Cao X, Chen D. 2005. The BMP signaling and in vivo bone formation. Gene 357:1–8.

Davydova J, Le LP, Gavrikova T, Wang M, Krasnykh V, Yamamoto M. 2004. Infectivity-enhanced cyclooxygenase-2-based conditionally replicative adenoviruses for esophageal adenocarcinoma treatment. Cancer Res 64:4319–4327.

Giannoudis PV, Kanakaris NK, Einhorn TA. 2007. Interaction of bone morphogenetic proteins with cells of the osteoclast lineage: Review of the existing evidence. Osteoporos Int 18:1565–1581.

Itoh K, Udagawa N, Katagiri T, Iemura S, Ueno N, Yasuda H, Higashio K, Quinn JM, Gillespie MT, Martin TJ, Suda T, Takahashi N. 2001. Bone morphogenetic protein 2 stimulates osteoclast differentiation and survival supported by receptor activator of nuclear factor-kappaB ligand. Endocrinology 142:3656–3662.

Jensen ED, Pham L, Billington CJ, Jr., Espe K, Carlson AE, Westendorf JJ, Petryk A, Gopalakrishnan R, Mansky KC. 2010. Bone morphogenetic protein 2 directly enhances differentiation of murine osteoclast precursors. J Cell Biochem 109:672–682.

Kanatani M, Sugimoto T, Kaji H, Kobayashi T, Nishiyama K, Fukase M, Kumegawa M, Chihara K. 1995. Stimulatory effect of bone morphogenetic protein-2 on osteoclast-like cell formation and bone-resorbing activity. J Bone Miner Res 10:1681–1690.

Kaneko H, Arakawa T, Mano H, Kaneda T, Ogasawara A, Nakagawa M, Toyama Y, Yabe Y, Kumegawa M, Hakeda Y. 2000. Direct stimulation of osteoclastic bone resorption by bone morphogenetic protein (BMP)-2 and expression of BMP receptors in mature osteoclasts. Bone 27:479–486.

Kirker-Head CA, Boudrieau RJ, Kraus KH. 2007. Use of bone morphogenetic proteins for augmentation of bone regeneration. J Am Vet Med Assoc 231:1039–1055.

Larrain J, Oelgeschlager M, Ketpura NI, Reversade B, Zakin L, De Robertis EM. 2001. Proteolytic cleavage of chordin as a switch for the dual activities of Twisted gastrulation in BMP signaling. Development 128:4439–4447.

Lieberman JR, Daluiski A, Einhorn TA. 2002. The role of growth factors in the repair of bone. Biology and clinical applications. J Bone Joint Surg Am 84-A:1032–1044.

MacKenzie B, Wolff R, Lowe N, Billington CJ, Jr., Peterson A, Schmidt B, Graf D, Mina M, Gopalakrishnan R, Petryk A. 2009. Twisted gastrulation limits apoptosis in the distal region of the mandibular arch in mice. Dev Biol 328:13–23.

Nohe A, Keating E, Knaus P, Petersen NO. 2004. Signal transduction of bone morphogenetic protein receptors. Cell Signal 16:291–299.

Nosaka T, Morita S, Kitamura H, Nakajima H, Shibata F, Morikawa Y, Kataoka Y, Ebihara Y, Kawashima T, Itoh T, Ozaki K, Senba E, Tsuji K, Makishima F, Yoshida N, Kitamura T. 2003. Mammalian twisted gastrulation is essential for skeleto-lymphogenesis. Mol Cell Biol 23:2969–2980.

Oelgeschlager M, Reversade B, Larrain J, Little S, Mullins MC, De Robertis EM. 2003. The pro-BMP activity of Twisted gastrulation is independent of BMP binding. Development 130:4047–4056.

Okamoto M, Murai J, Yoshikawa H, Tsumaki N. 2006. Bone morphogenetic proteins in bone stimulate osteoclasts and osteoblasts during bone development. J Bone Miner Res 21:1022–1033.

Petryk A, Anderson RM, Jarcho MP, Leaf I, Carlson CS, Klingensmith J, Shawlot W, O'Connor MB. 2004. The mammalian twisted gastrulation gene functions in foregut and craniofacial development. Dev Biol 267:374–386.

Petryk A, Shimmi O, Jia X, Carlson AE, Tervonen L, Jarcho MP, O'Connor MB, Gopalakrishnan R. 2005. Twisted gastrulation and chordin inhibit differentiation and mineralization in MC3T3-E1 osteoblast-like cells. Bone 36:617–626.

Porter AG, Janicke RU. 1999. Emerging roles of caspase-3 in apoptosis. Cell Death Differ 6:99–104.

Rodan GA, Martin TJ. 2000. Therapeutic approaches to bone diseases. Science 289:1508–1514.

Rodriguez JS, Mansky KC, Jensen ED, Carlson AE, Schwarz T, Pham L, Mackenzie B, Prasad H, Rohrer MD, Petryk A, Gopalakrishnan R. 2009. Enhanced osteoclastogenesis causes osteopenia in Twisted gastrulation-deficient mice through increased BMP signaling. J Bone Miner Res 24: 1917–1926.

Ross JJ, Shimmi O, Vilmos P, Petryk A, Kim H, Gaudenz K, Hermanson S, Ekker SC, O'Connor MB, Marsh JL. 2001. Twisted gastrulation is a conserved extracellular BMP antagonist. Nature 410:479–483.

Toth JM, Boden SD, Burkus JK, Badura JM, Peckham SM, McKay WF. 2009. Short-term osteoclastic activity induced by locally high concentrations of recombinant human bone morphogenetic protein-2 in a cancellous bone environment. Spine (PhilaPa 1976) 34:539–550.

Vaananen HK, Laitala-Leinonen T. 2008. Osteoclast lineage and function. Arch Biochem Biophys 473:132–138.

Xiao G, Gopalakrishnan R, Jiang D, Reith E, Benson MD, Franceschi RT. 2002. Bone morphogenetic proteins, extracellular matrix, and mitogen-activated protein kinase signaling pathways are required for osteoblast-specific gene expression and differentiation in MC3T3-E1 cells. J Bone Miner Res 17:101–110.